# Structure of two-dimensional plasma crystals in anharmonic Penning traps

Daniel H. E. Dubin
*Department of Physics, University of California at San Diego, La Jolla, California 92093, USA*
(Received 21 May 2013; published 8 July 2013)

This paper derives an analytic expression for the density per unit area of charges confined in a two-dimensional configuration in a Penning trap with an anharmonic applied trap potential that is expressed as a multipole expansion. This expression is used to find the optimum potential, with a given number of multipoles, for trapping a plasma with the most uniform possible density per unit area. Minimum energy states in such an optimized trap potential are evaluated numerically and the resulting crystal structures are shown to be defect-free over the central region of the plasma where the density is most nearly uniform. The paper also briefly considers the possibility of using an $\ell = 3$ rotating wall trap potential in order to confine minimum energy states with triangular symmetry and no defects.

DOI: 10.1103/PhysRevA.88.013403 PACS number(s): 37.10.Ty, 52.27.Gr, 52.27.Jt

## I. INTRODUCTION

In several recent experiments charged particles have been trapped and cooled in two-dimensional configurations using a Penning trap. These configurations have been used to study structural phase transitions [1], plasma waves and wakes [2], qubit error correction in quantum computing [3], and quantum simulations of the hexagonal two-dimensional (2D) Ising model with long-range interactions [4]. In the experiments the external trap potential, produced by voltages on cylindrically symmetric electrodes, is carefully crafted to be a nearly pure quadrupole:

$$\phi_{\rm trap}(\rho,z) = \frac{1}{2}\frac{m\omega_z^2}{q}\left(z^2 - \frac{1}{2}\rho^2\right), \tag{1}$$

where $\rho$ and $z$ are cylindrical coordinates and $\omega_z$ is the axial trap frequency. Such traps produce harmonic oscillations for a single particle in the trap and so are often referred to as harmonic traps. In this paper we consider the effect on the 2D plasma equilibrium of adding higher-order multiple moments to the trap potential. We find that these higher-order multipoles can be employed to manipulate the areal (2D) density of the plasma crystal so as to produce a more uniform and defect-free 2D crystalline structure than is possible in a harmonic trap. In linear RF traps, it has been shown that adding anharmonic terms to the trap potential could generate uniformly spaced strings of ions, which have some potential benefits for quantum computation [5]. Two-dimesional lattices with fewer defects could make closer contact to the hexagonal 2D Ising model and may also provide a more stable crystal structure that allows better imaging and addressing of individual ions in quantum-computing applications [6,7].

Equilibria for $N \gg 1$ charges confined in a harmonic trap have been carefully studied previously [8]. The charges form a uniform density spheroid whose density is set by the plasma rotation frequency and cyclotron frequency, and whose aspect ratio (i.e., length/diameter) depends on the relative strength of the trap potential (parametrized by $\omega_z$) compared to the potential produced by the plasma charges (as parametrized by the plasma frequency $\omega_p$). As $\omega_z/\omega_p$ tends toward the maximum value of unity, the aspect ratio tends to zero, and the charges form a 2D equilibrium in the $z = 0$ plane. For $N \gg 1$, the value of $\omega_z/\omega_p$ must satisfy

$$1 - \frac{\omega_z^2}{\omega_p^2} < \frac{1.33}{N^{1/2}}, \quad N \gg 1, \tag{2}$$

to achieve the 2D equilibrium; otherwise the self electric field of the plasma pushes ions out of the $z = 0$ plane. The number of charges per unit area in the equilibrium, $\sigma$, is the projection of the uniform spheroid onto $z = 0$ and hence is roughly proportional to $\sqrt{1-\rho^2/r_p^2}$, where $r_p$ is the plasma radius. This nonuniform density per unit area produces 2D laser-cooled crystal structures with many dislocations, because the interparticle spacing in the 2D crystal increases with radius $\rho$ [9]. However, we show that higher-order multipole moments added to the trap potential can make $\sigma$ more uniform with radius, producing more symmetric crystals.

## II. TRAP POTENTIAL

In this paper we are concerned with Penning trap plasma equilibria wherein the total force on each particle is zero, as seen in a frame rotating with the plasma. This force can be written as the gradient of a potential,

$$\mathbf{F}(\mathbf{r}_i) = -\nabla q\phi_{\rm eff}(\mathbf{r}_i), \tag{3}$$

where the effective potential $q\phi_{\rm eff}$ of charge a $q$ with mass $m$ at position $\mathbf{r}_i$, as seen in a frame rotating at frequency $\omega$ with the plasma, is a sum of three terms [8]:

$$q\phi_{\rm eff}(\mathbf{r}_i) = q\phi_{\rm trap}(\rho_i,z_i) + \tfrac{1}{4}m\,\omega_p^2\rho_i^2 + q\phi_p(\mathbf{r}_i)\,. \tag{4}$$

Here $q\phi_p(\mathbf{r}_i)$ is the electrostatic potential energy of charge $i$ due to the other plasma charges (as well as image charges in the trap electrodes), the term proportional to $\rho^2$ is the effective potential well from plasma rotation at frequency $\omega$, the plasma frequency $\omega_p$ is related to $\omega$ by $\omega_p^2 = 2\omega(\Omega_c - \omega)$, and $\Omega_c$ is the cyclotron frequency.

For a plasma whose radius $r_p$ is small compared to the electrode radius $r_w$, it is useful to express $q\phi_{\rm trap}(\rho,z)$ as a multipole expansion:

$$q\phi_{\rm trap}(\rho,z) = \sum_{n=0}^{\infty} V_{2n}\left(\frac{r}{r_w}\right)^{2n} P_{2n}\left(\frac{z}{r}\right), \tag{5}$$

 

where $P_n(x)$ is a Legendre polynomial, $r = \sqrt{\rho^2 + z^2}$ is spherical radius, and the multipole coefficients $V_{2n}$ are determined by the applied electrode voltages. [We assume the trap potential is an even function of $z$, so that only even multipoles enter Eq. (5).] For an ideal harmonic trap, multipoles with $2n > 2$ are zero by choice of the electrode geometry and applied voltages. Then $V_2 = (1/2)\,m\omega_z^2 r_w^2$ and $q\phi_{\rm trap}$ has the quadrupolar (harmonic) form of Eq. (1). Here, however, we consider plasmas in anharmonic traps, where the trap potential includes the higher multipole moments $V_{2n}$. We find it useful to express these moments in terms of dimensionless coefficients $C_{2n} = r_p^{2n-2} V_{2n}/(r_w^{2n-2} V_2)$, writing Eq. (5) as

$$\begin{aligned} q\phi_{\rm trap}(\rho,z) &= V_0 + \frac{1}{2}m\omega_z^2 r_p^2 \sum_{n=1}^{\infty} C_{2n}\left(\frac{r}{r_p}\right)^{2n} P_{2n}\left(\frac{z}{r}\right) \\ &= V_0 + \frac{1}{2}m\omega_z^2 r_p^2\left[\overline{z}^2 - \frac{1}{2}\overline{\rho}^2\right. \\ &\quad + C_4\left(\overline{z}^4 - 3\overline{z}^2\overline{\rho}^2 + \frac{3}{8}\overline{\rho}^4\right) \\ &\quad \left. + C_6\left(\overline{z}^6 - \frac{15}{2}\overline{z}^4\overline{\rho}^2 + \frac{45}{8}\overline{z}^2\overline{\rho}^4 - \frac{5}{16}\overline{\rho}^6\right) + \cdots\right], \end{aligned} \tag{6}$$

where $\overline{z} = z/r_p$ and $\overline{\rho} = \rho/r_p$.

## III. 2D FLUID EQUILIBRIUM

We focus on equilibria in this trap potential produced by a sufficiently large value of $\omega_z$ so that the plasma is a thin plane of charge trapped in the $z = 0$ plane, with number per area $\sigma(\rho,\theta)$. For $N$ identical charges at positions $(\rho_i,\theta_i)$, $\sigma$ is given by

$$\sigma(\rho,\theta) = \sum_{i=1}^{N} \frac{\delta(\rho-\rho_i)\delta(\theta-\theta_i)}{\rho}. \tag{7}$$

The potential energy $q\phi_p(\rho_i,\theta_i)$ for a charge located at $(\rho_i,\theta_i)$ due to other charges can then be obtained from $\sigma$ using a Green's function solution of Poisson's equation,

$$\begin{aligned} q\phi_p(\rho_i,\theta_i) &= q^2 \sum_{j\neq i} G(\rho_i,\rho_j,\theta_i-\theta_j) \\ &\quad + \lim_{\varepsilon\to 0}[q^2 G(\rho_i,\rho_i+\varepsilon,0) - q^2/\varepsilon] \\ &= \lim_{\varepsilon\to 0} q^2 \int \rho_o\, d\rho_0\, d\theta_0 G(\rho_i,\rho_0+\varepsilon,\theta_i-\theta_0) \\ &\quad \times \sigma(\rho_0,\theta_0) - q^2/\varepsilon, \end{aligned} \tag{8}$$

where the Green's function $G$ satisfies

$$\nabla^2 G = -4\pi\delta(z)\frac{\delta(\rho-\rho_0)}{\rho}\delta(\theta-\theta_0) \tag{9}$$

with the boundary condition that $G = 0$ on the electrodes. (The last term and the $\varepsilon \to 0$ limit in Eq. (8) are employed in order to account for the interaction energy of a charge with its own image, $\lim_{\varepsilon\to 0}[q^2 G(\rho_i,\rho_i+\varepsilon,0) - q^2/\varepsilon]$ [10].)

If $r_w \gg r_p$, so that image charges can be neglected when determining $\phi_p$, one can use the free-space Green's function, which has the following useful form:

$$\lim_{r_w\to\infty} G(\rho,\rho_0,\Delta\theta) = \sum_{\ell=-\infty}^{\infty} e^{i\ell\Delta\theta}\int_0^{\infty} dk\, J_\ell(k\rho)J_\ell(k\rho_0), \tag{10}$$

where $J_\ell(x)$ is a Bessel function of the first kind.

For a trap potential with given multipole coefficients $C_{2n}$, $\sigma$ is determined by finding a charge configuration with $\mathbf{F}(\mathbf{r}_i) = \mathbf{0}$ for each charge.

For $N$ point charges, this procedure can be carried out numerically, and the results of such calculations are presented in Sec. VI. However, if we approximate $\sigma(\rho,\theta)$ as a smooth function of position $\overline{\sigma}(\rho)$ (a mean-field or fluid theory, useful in the $N \gg 1$ limit), then analytic expressions for the equilibrium form of $\overline{\sigma}(\rho)$ can be obtained. These expressions rely on the following integral identities:

$$\begin{aligned} I_{2n} &\equiv 2\pi\int_0^1 \overline{\rho}_0 d\overline{\rho}_0 \int_0^{\infty} dk\, J_0(k\overline{\rho})J_0(k\overline{\rho}_0)\sqrt{1-\overline{\rho}_0^2}\,\overline{\rho}_0^{2n} \\ &= \sum_{k=0}^{n+1} \phi_{2n,k}\overline{\rho}^{2k}, \end{aligned} \tag{11}$$

where $0 < \overline{\rho} < 1$ is assumed.

A list of the coefficients $\phi_{2n,k}$ is given in Table I. Using these identities, we obtain the following expression for the equilibrium mean-field density per unit area $\overline{\sigma}(\overline{\rho})$:

$$\overline{\sigma}(\overline{\rho}) = \sqrt{1-\overline{\rho}^2}\sum_{n=0}^{\infty}\sigma_{2n}\overline{\rho}^{2n}, \tag{12}$$

where the coefficients $\sigma_{2n}$ are chosen so that the force on the plasma vanishes. Using Eqs. (8) and (10)–(12), and neglecting the self-image charge potential, the plasma potential inside the plasma can be written as a power series in $\rho$:

$$q\phi_p(\rho) = q^2 r_p \sum_{n=0}^{\infty}\sigma_{2n}\sum_{k=0}^{n+1}\phi_{2n,k}\overline{\rho}^{2k}. \tag{13}$$

The mean-field equilibrium condition is $q\phi_{\rm eff}(\rho,z=0) =$ constant inside the planar plasma. Using Eqs. (4), (6), and (13), this equilibrium requirement can be written as

$$\begin{aligned} &\frac{1}{2}m\omega_\perp^2 r_p^2\left(\overline{\rho}^2 + \sum_{n=2}^{\infty}\overline{C}_{2n}P_{2n}(0)\overline{\rho}^{2n}\right) \\ &\quad + q^2 r_p\sum_{n=0}^{\infty}\sigma_{2n}\sum_{k=0}^{n+1}\phi_{2n,k}\overline{\rho}^{2k} = \text{constant}, \end{aligned} \tag{14}$$

where $\omega_\perp^2 \equiv \beta\omega_z^2$ is the perpendicular trap frequency, $\overline{C}_{2n} \equiv C_{2n}/\beta$, and we have introduced the trap parameter $\beta$ via the

TABLE I. The integral $I_{2n}(\overline{\rho})$.

| $2n$ | $I_{2n}(\overline{\rho})$ |
|---|---|
| 0 | $\frac{\pi^2}{4}(2-\overline{\rho}^2)$ |
| 2 | $\frac{\pi^2}{64}(8+8\overline{\rho}^2-9\overline{\rho}^4)$ |
| 4 | $\frac{\pi^2}{256}(16+8\overline{\rho}^2+18\overline{\rho}^4-25\overline{\rho}^6)$ |
| 6 | $\frac{\pi^2}{16\,384}(640+256\overline{\rho}^2+288\overline{\rho}^4+800\overline{\rho}^6-1225\overline{\rho}^8)$ |
| 8 | $\frac{\pi^2}{65\,536}(1792+640\overline{\rho}^2+576\overline{\rho}^4+800\overline{\rho}^6+2450\overline{\rho}^8-3969\overline{\rho}^{10})$ |

definition [8]

$$\beta \equiv \frac{\omega_p^2}{2\omega_z^2} - \frac{1}{2} = \frac{\omega(\Omega_c - \omega)}{\omega_z^2} - \frac{1}{2}. \tag{15}$$

For a harmonic trap, the trap parameter must be greater than zero in order for there to be a radial potential well that confines the plasma charges.

Equation (14) can be solved for the density coefficients $\sigma_{2n}$ by collecting powers of $\overline{\rho}$. Noting that $P_{2n}(0) = \sqrt{\pi}/[\Gamma(n+1)\Gamma(1/2-n)]$, and using Table I, we obtain, after some algebra,

$$\sigma_0 = \frac{2}{\pi^2}\frac{r_p}{a_0^3}\left(1 + \frac{1}{3}\overline{C}_4 - \frac{3}{10}\overline{C}_6 + \frac{2}{7}\overline{C}_8 - \frac{5}{18}\overline{C}_{10} + \cdots\right), \tag{16}$$

$$\sigma_2 = \frac{4}{3\pi^2}\frac{r_p}{a_0^3}\left(\overline{C}_4 - \frac{3}{5}\overline{C}_6 + \frac{18}{35}\overline{C}_8 - \frac{10}{21}\overline{C}_{10} + \cdots\right), \tag{17}$$

$$\sigma_4 = -\frac{8}{5\pi^2}\frac{r_p}{a_0^3}\left(\overline{C}_6 - \frac{4}{7}\overline{C}_8 + \frac{10}{21}\overline{C}_{10} + \cdots\right), \tag{18}$$

$$\sigma_6 = \frac{64}{35\pi^2}\frac{r_p}{a_0^3}\left(\overline{C}_8 - \frac{5}{9}\overline{C}_{10}\cdots\right), \tag{19}$$

$$\sigma_8 = -\frac{128}{63\pi^2}\frac{r_p}{a_0^3}(\overline{C}_{10} + \cdots), \tag{20}$$

and so on, where the scale length $a_0 \equiv (q^2/m\omega_\perp^2)^{1/3}$ is on the order of the interparticle spacing. Note that for $r_p/r_w \ll 1$, the scaled multipole coefficients $\overline{C}_{2n}$ of the trap potential fall off rapidly with increasing $n$, as $(r_p/r_w)^{2n-2}$, so these series expressions tend to converge rapidly. Also, note that if $\overline{C}_{2n} = 0$ for $n > M$, then $\sigma_{2n} = 0$ for $n \geqslant M$. For instance, in a pure harmonic trap with $\overline{C}_4 = \overline{C}_6 = \cdots = 0$ only $\sigma_0$ is nonzero, and the mean-field density is [11]

$$\overline{\sigma}(\overline{\rho}) = \frac{2r_p}{\pi^2 a_0^3}\sqrt{1-\overline{\rho}^2}. \tag{21}$$

The plasma radius $r_p$ is determined by the total particle number $N$ and the multipole coefficients via the expression

$$N = 2\pi r_p^2 \int_0^1 \overline{\rho}\, d\overline{\rho}\, \overline{\sigma}(\overline{\rho}) = \frac{\pi^{3/2}}{2} r_p^2 \sum_{n=0}^{\infty} \sigma_{2n} \frac{\Gamma(n+1)}{\Gamma(n+5/2)}, \tag{22}$$

where we have used Eq. (12).

Substituting from Eqs. (16)–(20) and collecting terms yields

$$N = \frac{4}{3\pi}\frac{r_p^3}{a_0^3}\left(1 + \frac{3}{5}\overline{C}_4 - \frac{9}{14}\overline{C}_6 + \frac{2}{3}\overline{C}_8 - \frac{15}{22}\overline{C}_{10} + \cdots\right). \tag{23}$$

Note that for given multipole moments, this implies that the plasma radius scales as $N^{1/3}$. One might have naively expected that the plasma radius would scale as $N^{1/2}$, but this scaling assumes a mean areal density that is independent of $N$. However, for fixed external potentials Eqs. (16)–(20) imply that the mean areal density increases as $N$ increases (as $N^{1/3}$), so that the radius increases more slowly than $N^{1/2}$.

For anharmonic traps, the criterion for stability of a 2D equilibrium, Eq. (2), must be modified. This equation is based on the stability criterion for a uniform 2D crystal, that $\sigma(4\pi q^2/m\omega_{z_h}^2)^{2/3} < w_1 \equiv 1.11\ldots$, where $\sigma$ is the density per unit area and $\omega_{z_h}$ is the harmonic trap frequency [11]. In an anharmonic trap the effective harmonic frequency depends on radius; according to Eq. (6), it is given by $\omega_{z_h}^2 = \omega_z^2[1 - 3C_4\overline{\rho}^2 + (45/8)\,C_6\overline{\rho}^4 + \cdots]$. However, if $\overline{C}_4$, $\overline{C}_6, \ldots$ are of order unity, then $C_4, C_6, \ldots$ are small (of order $\beta \ll 1$), so this radial variation in the harmonic frequency can be neglected, and one can take $\omega_{z_h}^2 = \omega_z^2$. The areal density $\sigma$ also varies with radius, but for simplicity we assume that anharmonic terms are such that the maximum, $\sigma_0$, occurs at $\overline{\rho} = 0$. Using Eq. (16) for $\sigma_0$ and Eq. (23) for $r_p$ then yields the following stability criterion for a 2D equilibrium with $N \gg 1$:

$$\beta < \left(\frac{\pi^3\omega_1^3}{96N}\right)^{1/2} \frac{[1 + (3/5)\overline{C}_4 - (9/14)\overline{C}_6 + (2/3)\overline{C}_8 - (15/22)\overline{C}_{10}\ldots]^{1/2}}{[1 + (1/3)\overline{C}_4 - (3/10)\overline{C}_6 + (2/7)\overline{C}_8 - (5/18)\overline{C}_{10}\ldots]^{3/2}}. \tag{24}$$

Using Eq. (15) to relate $\beta$ to $\omega_p^2/\omega_z^2$, this criterion reduces to Eq. (2) in the harmonic limit $\overline{C}_4 = \overline{C}_6 = \cdots = 0$.

## IV. IMAGE CHARGES

So far, the effect of images charges on the equilibrium has been neglected. To lowest order in $r_p/r_w$, this effect can be evaluated by approximating the plasma as a monopole with charge $Nq$ located at the origin, which produces image charges on the wall that create an extra multipole image potential of the form given in Eq. (5). Hence, there is a correction to the coefficients $V_{2n}$ in Eq. (5) due to the image charge, with an order of magnitude of $Nq^2/r_w$ [12]. For example, for a trap with cylindrical electrodes, the image charge potential created by a charge $Nq$ located at the origin is

$$q\phi^{\text{image}}(\rho,z) = -\frac{Nq^2}{r_w}\int_{-\infty}^{\infty}\frac{dk}{\pi}\frac{K_0(|k|)}{I_0(|k|)}I_0\left(|k|\frac{\rho}{r_w}\right)e^{ikz/r_w}. \tag{25}$$

Taylor expansion of $\phi^{\text{image}}$ for $\rho$ and $z$ near the origin yields a multipole expansion of $\phi^{\text{image}}$ with the same form as Eq. (5), with coefficients $V_{2n}^{\text{image}}$ given by

$$V_{2n}^{\text{image}} = -\frac{Nq^2}{r_w}\frac{(-1)^n}{(2n)!}\int_{-\infty}^{\infty}\frac{dk}{\pi}k^{2n}\frac{K_0(|k|)}{I_0(|k|)}. \tag{26}$$

TABLE II. Image charge multipole coefficients for a cylindrical wall.

| $2n$ | $V_{2n}^{\text{image}}/(Nq^2/r_w)$ |
|---|---|
| 2 | 0.205 91 |
| 4 | −0.054 905 |
| 6 | 0.014 296 |
| 8 | −0.003 658 2 |
| 10 | $9.2745 \times 10^{-4}$ |

The coefficients $V_{2n}^{\text{image}}$ are given in Table II.

## V. UNIFORM DENSITY MEAN-FIELD EQUILIBRIUM

For a harmonic trap, the charge density $\overline{\sigma}(\overline{\rho})$, given by Eq. (21), is strongly nonuniform. For studies that involve 2D plasma crystals the nonuniformity of $\overline{\sigma}(\overline{\rho})$ produces inhomogeneous crystal structures with many dislocations throughout the crystal. By choosing appropriate multipole coefficients $\overline{C}_4, \overline{C}_6, \ldots$, the charge density can be made more uniform, which allows a more symmetric crystal structure.

For instance, if we assume $\overline{C}_4 \neq 0$ but $\overline{C}_{2n} = 0$ for $2n > 4$, then according to Eqs. (12) and (16) and (17),

$$\overline{\sigma}(\overline{\rho}) = \sqrt{1-\overline{\rho}^2}\,(\sigma_0 + \sigma_2\overline{\rho}^2)\,. \tag{27}$$

If we choose $\overline{C}_4$ so that $\sigma_2 = \sigma_0/2$, then $\overline{\sigma}''(0) = 0$, making the charge density as uniform as possible in this case. According to Eqs. (16) and (17), $\sigma_2 = \sigma_0/2$ provided that $\overline{C}_4 = 1$, or $C_4 = \beta$ and $V_4 = V_2\beta r_w^2/r_p^2$. (Since $\beta \ll 1$ for a 2D planar crystal with $N \gg 1$ [see Eq. (24)], this implies that $V_4$ need not be much larger than $V_2$ even if $r_w \gg r_p$.) For $\overline{C}_4 = 1$ the plasma radius $r_p$ is determined by the number of charges through Eq. (23):

$$r_p^3 = \frac{15\pi}{32} N a_0^3. \tag{28}$$

By adding a $\overline{C}_6$ moment, the areal density can be made even more uniform. Equations (12) and (16)–(18) imply that now

$$\overline{\sigma}(\overline{\rho}) = \sqrt{1-\overline{\rho}^2}(\sigma_0 + \sigma_2\overline{\rho}^2 + \sigma_4\overline{\rho}^4). \tag{29}$$

Choosing $\sigma_2 = \sigma_0/2$ and $\sigma_4 = 3\sigma_0/8$ sets both $\sigma''(0)$ and $\sigma^{iv}(0)$ equal to zero. According to Eqs. (16)–(18), these values for $\sigma_2$ and $\sigma_4$ are obtained when $\overline{C}_4 = -\overline{C}_6 = 2/3$, which implies $V_4 = 2/3 V_2\beta\, r_w^2/r_p^2$ and $V_6 = -2/3 V_2\beta\, r_w^4/r_p^4$. (Unless $V_2$ is fairly small this large value for $V_6$ may be difficult to achieve in a realistic geometry with $r_w \gg r_p$.) For these values of $\overline{C}_4$ and $\overline{C}_6$ the plasma radius is determined in terms of $N$ by Eq. (23):

$$r_p^3 = \frac{105\pi}{256} N a_0^3\,. \tag{30}$$

Keeping even higher multipoles allows even more uniform $\overline{\sigma}(\overline{\rho})$, but this is probably impractical due to the large electrode potentials required. Nevertheless, for completeness, we note that the "best case" (in some sense) would be perfectly uniform charge density, $\overline{\sigma}(\overline{\rho}) = \overline{\sigma}_0$, out to radius $r_p$. According to Eq. (8) this produces a plasma potential given by

$$\phi_{\text{plasma}}(\overline{\rho}) = 4q^2\overline{\sigma}_0 r_p\, E(\overline{\rho}^2), \quad \overline{\rho} < 1, \tag{31}$$

where $E(x)$ is an elliptic integral. The required trap potential is the negative of this (up to an additive constant), requiring multipoles of all orders. Taylor expansion of Eq. (31) to second order in $\overline{\rho}$ implies that $m\omega_\perp^2 r_p = \pi q^2\overline{\sigma}_0$. Also, since the areal density is uniform, $N = \pi r_p^2\overline{\sigma}_0$, so $r_p^3 = N a_0^3$. Note that $E'(x) \to \infty$ as $x \to 1$, implying that impossibly large trap electric fields would be needed at the plasma edge to achieve this uniform charge density configuration.

## VI. CRYSTAL STRUCTURE FOR PLANAR PLASMAS

In this section we examine the crystal structure of a collection of $N$ identical point charges cooled to a minimum energy state in the $z = 0$ plane of an anharmonic trap, as compared to the structure in a harmonic trap. For the anharmonic trap, we choose the case where only $\overline{C}_4 \neq 0$ and

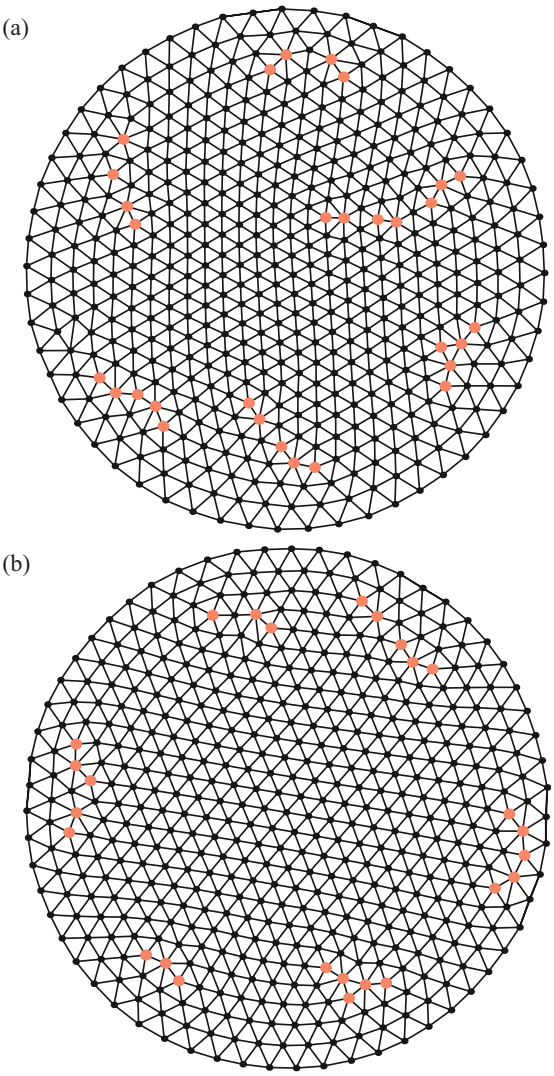


FIG. 1. (Color online) Local minimum energy state for $N = 500$ identical charges in (a) a harmonic trap ($\overline{C}_4 = 0$) and (b) an anharmonic trap with $\overline{C}_4 = 1$.

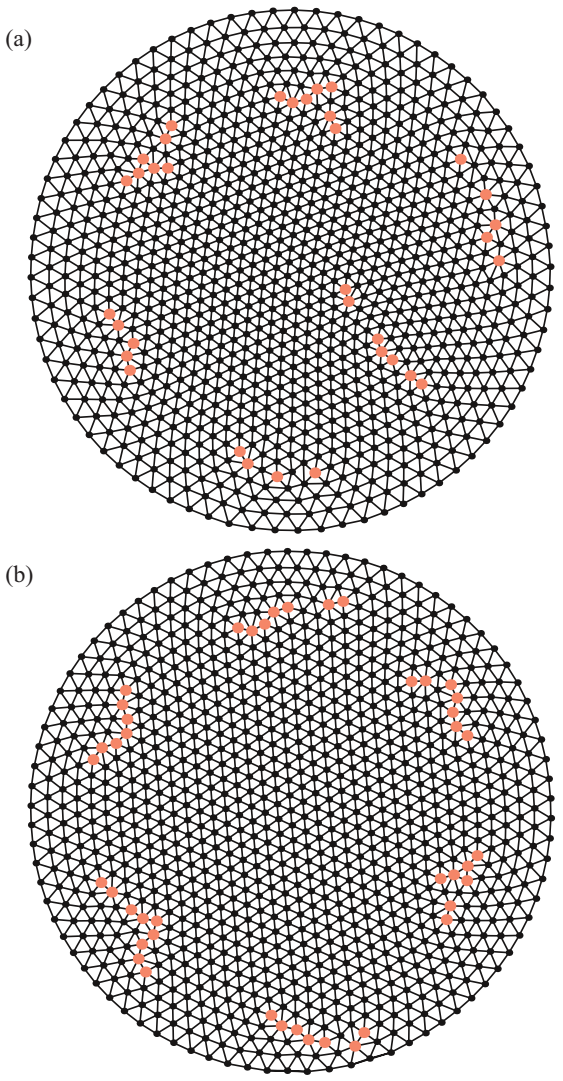


FIG. 2. (Color online) Local minimum energy state for $N = 1000$ identical charges in (a) a harmonic trap ($\overline{C}_4 = 0$) and (b) an anharmonic trap with $\overline{C}_4 = 1$.

minimize the following energy function:

$$\varepsilon = \sum_{i=1}^{N} \frac{1}{2} m\omega_\perp^2 \left( \rho_i^2 + \frac{3}{8} \overline{C}_4 \frac{\rho_i^4}{r_p^2} \right) + \sum_{i=2}^{N} \sum_{j=1}^{i-1} \frac{q^2}{|\mathbf{r}_i - \mathbf{r}_j|}. \quad (32)$$

We take $\overline{C}_4 = 0$ for a harmonic trap and $\overline{C}_4 = 1$ for the anharmonic trap with the most uniform density, with $r_p$ given by Eq. (28). For $N \gg 1$ there are many local energy minima. We attempt to find minima that are close to the absolute minimum by artificially cooling the charges very slowly via a Rosenbluth-Metropolis Monte-Carlo method [13]. We start with random initial positions at a coupling parameter $\Gamma \equiv q^2/a_0 T$ of 5 (where $T$ is the plasma temperature) and allow the system to equilibrate at this $\Gamma$ value for $10^4 N$ Monte Carlo steps, with step size chosen so that the acceptance ratio is in the range of 50%–70%. The $\Gamma$ value is then lowered in ten stages from 5 to 500, reducing the step size at each stage to keep the acceptance ratio roughly fixed, and equilibrating for $10^4 N$ steps at each stage. The value $\Gamma = 500$ is large enough so that particle positions vary from the local minimum by only a small fraction of an interparticle spacing. Finally, an energy minimization is performed via a conjugate gradient algorithm. The resulting 2D crystal structures are displayed in Fig. 1 for $N = 500$ and in Fig. 2 for $N = 1000$. In Figs. 1(a) and 2(a), $\overline{C}_4 = 0$, while in Figs. 1(b) and 2(b), $\overline{C}_4 = 1$. Lines are drawn between nearest neighbors using Voroni construction. Points shown in black have six nearest neighbors while those shown in red (gray) have either fewer or more than six, indicating dislocations in the crystal structure. For the harmonic trap, there are six sets of dislocations, roughly equally spaced in angle around the crystal. One of the six sets forms a seam running toward the center of the crystal. The seam is necessary in order to relieve stress in the crystal due to its nonuniformity. The nonuniformity is most easily observed in Figs. 3(a) and 4(a), which show the distance to the nearest neighbors for each charge plotted versus the radial position of the charge. This nearest-neighbor distance is smallest near the center and roughly follows the expected distance $d(\rho)$ based on a hexagonal lattice with mean-field density per unit area $\overline{\sigma}(\overline{\rho})$:

$$d(\overline{\rho}) = \sqrt{2/(\sqrt{3}\overline{\sigma}(\overline{\rho}))} \quad (33)$$

(the solid curve in the figures).

On the other hand, when $\overline{C}_4 = 1$ the crystal structure is considerably more uniform. There are still six sets of dislocations spaced evenly around the crystal, but they are closer to the edge, and there is no longer a radial seam of

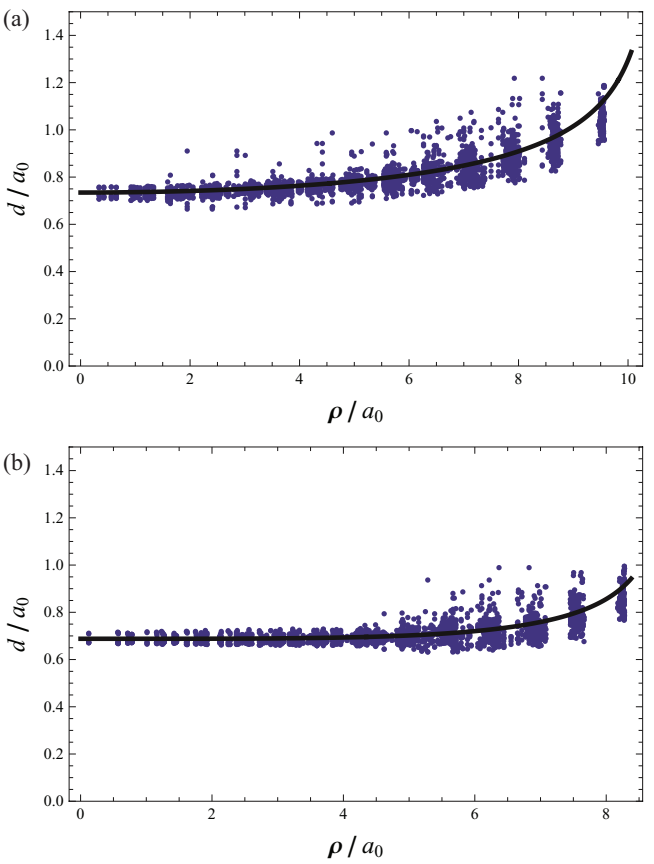


FIG. 3. (Color online) Nearest-neighbor distances versus radius for $N = 500$. The solid line represents the fluid theory. (a) $\overline{C}_4 = 0$. (b) $\overline{C}_4 = 1$.

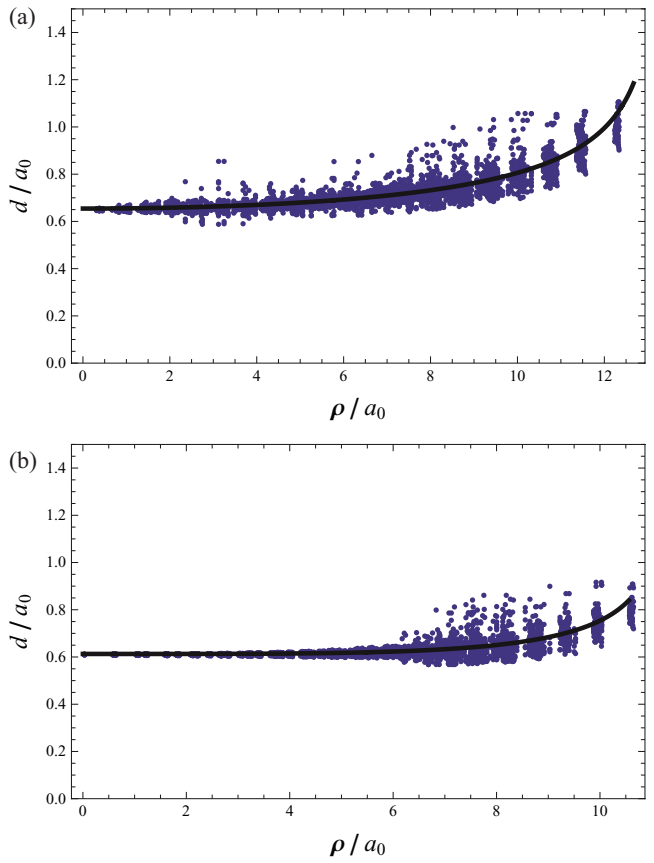


FIG. 4. (Color online) Nearest-neighbor distances versus radius for $N = 1000$. The solid line representes the fluid theory. (a) $\overline{C}_4 = 0$. (b) $\overline{C}_4 = 1$.

dislocations. The distance between nearest neighbors is also more uniform [Figs. 3(b) and 4(b)], as expected from Eq. (33), and displays far less scatter in the central region.

## VII. HIGHLY SYMMETRIC 2D CRYSTALS USING A ROTATING WALL POTENTIAL

In Penning trap experiments "rotating wall" potentials proportional to $\cos[\ell(\theta - \omega t)]$ are often applied via sectored external electrodes [14], in order to fix the plasma rotation frequency $\omega$. Typically, $\ell = 1$ or 2 rotating potentials are used for this purpose. However, an $\ell = 3$ potential has triangular symmetry that can be used to match the triangular symmetry of 2D hexagonal plasma crystals. With a properly chosen rotating wall strength, nearly perfect 2D hexagonal crystal structures can be obtained for particular values of $N$.

The energy function is now

$$\varepsilon = \sum_{i=1}^{N}\left[\frac{1}{2}m\omega_\perp^2\left(\rho_i^2 + \frac{3}{8}\frac{\rho_i^4}{r_p^2}\right) + \frac{V_{\rm wall}}{r_p^3}\rho_i^3\cos 3\theta_i\right] + \sum_{i=2}^{N}\sum_{j=1}^{i-1}\frac{q^2}{|\mathbf{r}_i - \mathbf{r}_j|}, \tag{34}$$

where we assume for simplicity that the rotating wall potential is produced by long sectored electrodes so as to have negligible $z$ dependence. Two examples of the resulting minimum energy

FIG. 5. (Color) 2D plasma crystal (blue dots) with $N = 21$ particles in an $\ell = 3$ rotating wall potential. Green dots are a perfect triangular lattice.

structures are displayed. In Fig. 5 with $N = 21$ particles, the displayed structure is attained for $V_{\rm wall} = 2.945q^2/a_0$. Blue dots show the equilibrium particle positions, while green dots show the positions for an exact triangular lattice. The second case with $N = 63$ particles, shown in Fig. 6, has the three vertex particles removed in order to improve the symmetry of the remaining charges. Here, $V_{\rm wall} = 5.154\,q^2/a_0$. Similar results can be obtained for even larger values of $N$, although for larger $N$ the crystal symmetry is not as well preserved.

For larger values of $V_{\rm wall}$, particles near the vertices are not confined due to a triangular separatrix in the external potential, caused by the rotating wall potential. Particles that cross the separatrix are lost. Such large rotating wall fields could be

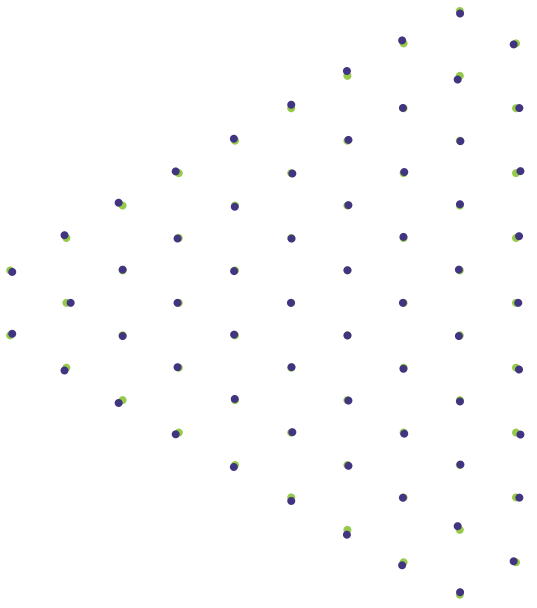

FIG. 6. (Color) Same as Fig. 5 but for $N = 63$ particles.

employed to remove particles from the plasma in a controlled fashion.

## VIII. DISCUSSION

This paper explores the utility of adding anharmonic terms to the external potential of a Penning trap in order to create 2D Coulomb crystals with more uniform structure than can be achieved in harmonic (quadrupole) Penning traps. When the trap potential is expressed as a cylindrically and axially symmetric multipole expansion, an analytic form for the mean-field density per unit area can be found. This analytic solution allows one to determine the optimum choice of multipole coefficients in order to obtain the most uniform possible mean-field density for a given set of multipoles. We find that numerically determined 2D crystal structures for $N \gg 1$ in such an optimized trap are dislocation-free 2D hexagonal lattices over the entire central region of the crystal, where the mean-field density is nearly uniform. However, there are still lattice dislocations in the edge region, in large part due to the circular crystal boundary that frustrates the hexagonal lattice. This can be alleviated by applying an $\ell = 3$ rotating wall potential which gives the boundary the necessary triangular symmetry to match the hexagonal lattice. In this case nearly perfect hexagonal lattices with no dislocations can be obtained.

Some open questions remain to be addressed in future work. For example, the linear normal modes of oscillation of the 2D crystals should be evaluated, as these modes can be utilized to diagnose and manipulate the plasma. The modes have been carefully studied for harmonic Penning traps [7,15], but will be modified by the additional multipole terms considered here. In addition, the stability of the crystal structure at finite temperature, the evolution of defects, and the 2D melting behavior all merit study as a function of trap anharmonicity. For Coulomb crystals in the $\ell = 3$ rotating wall fields discussed in Sec. VII, molecular dynamics simulations of particle loss across the separatrix could test the feasibility of using the separatrix to control particle number.

## ACKNOWLEDGMENTS

The author thanks Dr. John Bollinger for suggesting this topic and for useful discussions. This work is supported by NSF Grant No. PHY-0903877 and DOE Grant No. DE-SC0002451.

[1] T. B. Mitchell, J. J. Bollinger, D. H. E. Dubin, X.-P. Huang, W. M. Itano, and R. H. Baughman, Science **282**, 1290 (1998).
[2] J. M. Kriesel, J. J. Bollinger, T. B. Mitchell, L. B. King, and D. H. E. Dubin, Phys. Rev. Lett. **88**, 125003 (2002).
[3] M. J. Biercuk, H. Uys, A. P. VanDevender, N. Shiga, W. M. Itano, and J. J. Bollinger, Nature (London) **458**, 996 (2009).
[4] J. W. Britton, B. C. Sawyer, A. C. Keith, C.-C. J. Wang, J. K. Freericks, H. Uys, M. J. Biercuk, and J. J. Bollinger, Nature (London) **484**, 489 (2012).
[5] G. D. Lin, S.-L. Zhu, R. Islam, K. Kim, M.-S. Chang, S. Korenblit, C. Monroe, and L.-M. Duan, Europhys. Lett. **86**, 60004 (2009).
[6] J. D. Baltrusch, A. Negretti, J. M. Taylor, and T. Calarco, Phys. Rev. A **83**, 042319 (2011); D. Porras, J. I. Cirac, S. Kilina, S. Tretiak, and E. Einarsson, Phys. Rev. Lett. **96**, 250501 (2006).
[7] C.-C. Joseph Wang, A. C. Keith, and J. K. Freericks, Phys. Rev. A **87**, 013422 (2013).
[8] For a review, see D. H. E. Dubin and T. M. O'Neil, Rev. Mod. Phys. **71**, 87 (1999).
[9] V. M. Bedanov and F. M. Peeters, Phys. Rev. B **49**, 2667 (1994).
[10] See, for example, H. Wu, D. W. L. Sprung, and J. Martorell, Eur. J. Phys. **21**, 413 (2000).
[11] D. H. E. Dubin, Phys. Rev. Lett. **71**, 2753 (1993).
[12] M. D. Tinkle and S. Barlow, J. Appl. Phys. **90**, 1612 (2001).
[13] M. Newman and G. Barkema, *Monte Carlo Methods in Statistical Physics* (Clarendon, Oxford, 2001).
[14] F. Anderegg, E. M. Hollmann, and C. F. Driscoll, Phys. Rev. Lett. **81**, 4875 (1998); X.-P. Huang, J. J. Bollinger, T. B. Mitchell, W. M. Itano, and D. H. E. Dubin, Phys. Plasmas **5**, 1656 (1998).
[15] V. A. Schweigert and F. M. Peeters, Phys. Rev. B **51**, 7700 (1995).